Author Manuscript

Author Manuscript

Author Manuscript

Author Manuscript

HHS Public Access

Author manuscript

Int J Hyperthermia. Author manuscript; available in PMC 2024 February 05.

Published in final edited form as:

Int J Hyperthermia. 2023 ; 40(1): 2247187. doi:10.1080/02656736.2023.2247187.

Ultrasound-guided noninvasive pancreas ablation using histotripsy: feasibility study in an *in vivo* porcine model

Jessica Gannon[a], **Khan Mohammad Imran**[b,c], **Alissa Hendricks-Wenger**[a,b,c,d], **Michael Edwards**[e], **Hannah Covell**[a], **Lauren Ruger**[a], **Neha Singh**[f], **Margaret Nagai-Singer**[b], **Benjamin Tintera**[f], **Kristin Eden**[f], **Mishal Mendiratta-Lala**[g], **Joan Vidal-Jove**[h], **David Luyimbazi**[f,i], **Martha Larson**[j], **Sherrie Clark-Deener**[j], **Sheryl Coutermarsh-Ott**[b], **Irving C. Allen**[b,c,f,k], **Eli Vlaisavljevich**[a,c,k]

[a]Department of Biomedical Engineering and Mechanics, VA Tech, Blacksburg, VA, USA

[b]Department of Biomedical Sciences and Pathobiology, Virginia-MD College of Veterinary Medicine, Blacksburg, VA, USA

[c]Graduate Program in Translational Biology, Medicine and Health, Virginia Tech, Roanoke, VA, USA

[d]DeBusk College of Osteopathic Medicine, Lincoln Memorial University, Knoxville, TN, USA

[e]Department of Small Animal Clinical Sciences, Virginia-Maryland College of Veterinary Medicine, Blacksburg, VA, US

[f]Department of Basic Science Education, Virginia Tech Carilion School of Medicine, Roanoke, VA, USA

[g]Department of Radiology, MI Medicine, Ann Arbor, MI

[h]Interventional Oncology Institute Khuab, Comprehensive Tumor Center, Barcelona, Spain

[i]Department of Surgery, Carilion Clinic, Roanoke, VA, USA

[j]Department of Large Animal Clinical Sciences, Virginia-Maryland College of Veterinary Medicine, Blacksburg, VA, USA

[k]ICTAS Center for Engineering Health, Virginia Tech, Blacksburg, VA

Abstract

This is an Open Access article distributed under the terms of the Creative Commons Attribution-NonCommercial License (http://creativecommons.org/licenses/by-nc/4.0/), which permits unrestricted non-commercial use, distribution, and reproduction in any medium, provided the original work is properly cited. The terms on which this article has been published allow the posting of the Accepted Manuscript in a repository by the author(s) or with their consent.

CONTACT Eli Vlaisavljevich eliv@vt.edu Department of Biomedical Engineering and Mechanics, VA Tech, Blacksburg, VA, USA; Irving Coy Allen icallen@vt.edu Department of Biomedical Sciences and Pathobiology, Virginia-MD College of Veterinary Medicine, Blacksburg, VA, USA.

Disclosure statement

Author Dr. Eli Vlaisavljevich has an ongoing research partnership and financial relationship with HistoSonics, Inc. Author Dr. Joan Vidal-Jove is a consultant for Advanced Microbubbles Inc., for Chongqing Haifu Medical Technology Co. Ltd., and for HistoSonics, Inc. Author Lauren Ruger has an ongoing consulting relationship with Theraclion. No other authors have a conflict of interest to report.

Supplemental data for this article can be accessed online at https://doi.org/10.1080/02656736.2023.2247187.

Author Manuscript Author Manuscript Author Manuscript Author Manuscript

Pancreatic cancer is a malignant disease associated with poor survival and nearly 80% present with unresectable tumors. Treatments such as chemotherapy and radiation therapy have shown overall improved survival benefits, albeit limited. Histotripsy is a noninvasive, non-ionizing, and non-thermal focused ultrasound ablation modality that has shown efficacy in treating hepatic tumors and other malignancies. In this novel study, we investigate histotripsy for noninvasive pancreas ablation in a pig model. In two studies, histotripsy was applied to the healthy pancreas in 11 pigs using a custom 32-element, 500 kHz histotripsy transducer attached to a clinical histotripsy system, with treatments guided by real-time ultrasound imaging. A pilot study was conducted in 3 fasted pigs with histotripsy applied at a pulse repetition frequency (PRF) of 500 Hz. Results showed no pancreas visualization on coaxial ultrasound imaging due to overlying intestinal gas, resulting in off-target injury and no pancreas damage. To minimize gas, a second group of pigs ($n = 8$) were fed a custard diet containing simethicone and bisacodyl. Pigs were euthanized immediately ($n = 4$) or survived for 1 week ($n = 4$) post-treatment. Damage to the pancreas and surrounding tissue was characterized using gross morphology, histological analysis, and CT imaging. Results showed histotripsy bubble clouds were generated inside pancreases that were visually maintained on coaxial ultrasound ($n = 4$), with 2 pigs exhibiting off-target damage. For chronic animals, results showed the treatments were well-tolerated with no complication signs or changes in blood markers. This study provides initial evidence suggesting histotripsy's potential for noninvasive pancreas ablation and warrants further evaluation in more comprehensive studies.

Keywords

Pancreas; pancreatic cancer; histotripsy; large animal model; focused ultrasound

1. Introduction

Pancreatic cancer is considered a fatal malignancy with a 5-year overall survival rate of ~9%, with the majority of patients dying within 6 months of diagnosis [1]. Late-stage diagnosis, rapid local progression with vascular compromise, and metastasis all contribute to this high mortality rate [2]. The current gold standard treatment for pancreatic cancer is surgery [3]. However, the location of the tumor is a strong prognostic factor and may affect resectability. For instance, tumors involving vital vascular structures or tumors with local infiltration into the adjacent mesenteric fat present surgical challenges, precluding resection in a large number of patients [4]. Despite improved outcomes with the current standard of care, a high incidence of refractory disease from chemo- and radio-resistance, as well as local and distant recurrence, continue to pose significant treatment challenges [3].

There is a multitude of tumor ablation methods that have been considered for treating pancreatic cancer, including radiofrequency (RFA), microwave (MWA), cryoablation, high-intensity focused ultrasound (HIFU) thermal ablation, and irreversible electroporation (IRE) [5–7]. However, only HIFU and IRE have been developed as stand-alone or combination therapeutic options for pancreatic cancer, given the high complication risk and technical challenges associated with RFA and MWA, secondary to the retroperitoneal position of the pancreas and risk of thermal injury to the duct [8,9]. IRE and HIFU have shown some improvement over the standard of care in terms of morbidity, tissue conservation, improved

Author Manuscript Author Manuscript Author Manuscript Author Manuscript

surgical accessibility, and decreased hospitalization [10–12]. Additionally, IRE and HIFU treatments have shown improved overall survival with decreased tumor volumes [13,14]. However, like thermal ablation, these strategies can also be associated with significant complications. Although HIFU does not require needle puncture, it is a thermal-based modality, and thus thermal-induced ductal injury and the heat-sink effect can impact adequate local tumor control near critical structures. Pancreatic duct injury can result in a duct leak and severe pancreatitis or ductal stenosis with resultant obstructive pancreatitis [10]. IRE induces tissue destruction by the conduction of non-thermal electrical energy, which can preserve critical structures surrounding the targeted region. Unfortunately, electrical harmonics can be potentially hazardous with this modality, causing cardiac arrhythmias or muscle contractions [11,15]. The invasive needle puncture and the inability to treat large (>3 cm diameter) or multiple tumor nodules are additional limitations of IRE [11]. Additionally, the lack of real-time treatment feedback can limit the ability to create precise ablation zones. All these limitations render these treatment modalities challenging for clinical use [10,11]. As such, there remains an unmet need for a new ablation method that can overcome these limitations.

Histotripsy is a noninvasive, non-ionizing, and non-thermal focused ultrasound (US) ablation method that destroys tissue through the precise control of acoustic cavitation [16,17]. Unlike thermal HIFU, histotripsy disrupts tissue through mechanical effects (i.e., cavitation) [16]. Using high-pressure pulses applied by an external transducer, a cavitation “bubble cloud” is generated at a focal point on the target, and the expansion and collapse of the bubbles ablates the tissue into an acellular homogenate [16,18–20]. Due to the non-thermal nature of histotripsy, it does not have the limitations associated with thermal ablation [21,22]. For instance, histotripsy can produce consistent ablation in close proximity to major vessels with high accuracy, resulting in a “binary” treatment outcome, with millimeter precision and well-defined sharp boundaries (<2mm) [23–27]. Furthermore, histotripsy can preserve critical structures such as large vessels, bile ducts, and nerves due to the higher mechanical strength of these structures secondary to their collagenous histology [23–27]. Additional benefits include real-time imaging feedback [28] and the ability to cover tumor nodules of varying sizes and shapes [29]. Due to these features, histotripsy is currently being explored as a noninvasive ablation method for many applications in both preclinical and early clinical trials [30,31].

In this study, we investigate the feasibility of ultrasound-guided histotripsy for the noninvasive ablation of pancreatic tissue in an *in vivo* pig model. While prior studies highlight the potential of histotripsy for noninvasive tumor ablation in other organs, significant work remains to establish histotripsy’s potential in the pancreas. In addition to the unique challenges due to the tissue characteristics and risk of damage to nearby critical structures, the ability to visualize and precisely target the pancreas with histotripsy using ultrasound for real-time image guidance has inherent challenges secondary to the retroperitoneal position deep to the often gas-filled stomach. In this study, we investigate the feasibility of histotripsy for noninvasive pancreas ablation in an *in vivo* porcine model.

Author Manuscript Author Manuscript Author Manuscript Author Manuscript

2. Materials and methods

2.1. Animal model

A total of 11 male pigs (6–8 weeks old, 5–8 kg; Virginia Tech Swine Farm, Blacksburg, VA) were treated with histotripsy in this study. Once received, pigs were monitored three times during their first week to acclimate to their new housing, in accordance with Virginia Tech Institutional Animal Care and Use Committee (IACUC) protocols.

Two separate studies were conducted in this work to investigate the feasibility of histotripsy for targeting and ablating the pancreas *in vivo* under ultrasound guidance (Figure 1). In the first set of experiments, histotripsy was applied to the pancreas of 3 pigs that were fasted for 12 h prior to histotripsy to minimize intestinal contents and bowel gas (Figure 1(A)). All 3 pigs in this initial experiment were euthanized immediately after treatment. In the second set of experiments, histotripsy was applied to the pancreas of 8 pigs that were fed a special diet to attempt to minimize bowel gas, similar to that in prior studies evaluating HIFU in healthy pig pancreas [32] and human pancreas [33]. This speciality diet consisted of sweetened custard containing simethicone (2 ml/pig) and bisacodyl (0.3 mg/kg) which was fed to the pigs once daily for the 4 days prior to treatment to further minimize the intestinal contents and gas present on the day of treatment (Figure 1(B)). For this second round of experiments, 4 pigs were euthanized immediately after treatment and 4 pigs were survived for 1-week post-treatment. For all histotripsy treatments, animals were sedated by using an intramuscular injection of Telazol® (MWI Animal Health, USA), ketamine (MWI Animal Health, USA), and xylazine (MWI Animal Health, USA) at a dose of 2–4 mg/kg administered in 15-to-20-min intervals or when the animal began to demonstrate increased muscle tone or minimal purposeful movement. Anesthetized pigs were placed in a dorsal recumbent position on the surgical table with feet loosely restrained to maintain a stable position. The skin over the targeted tissue was shaved and treated with a depilatory cream (Naircare, Ewing, NJ, USA) for 10 min before removal with a wet towel. During treatment, the animal's heart rate, blood oxygen levels, respiratory rate, and temperature were monitored using Propaq Encore Vital Signs Monitor (Welch Allyn, Beaverton, Oregon, USA) by trained personnel. After treatment, animals were either immediately euthanized or recovered and returned to their housing for 1 week after treatment, as described above. For pigs recovered after treatment, the animals were visually monitored for 2–3 h in recovery kennels until fully recovered and then returned to their standard housing. After recovery, animals were monitored daily for general health to determine any changes in behavior, diet, and skin lesions. One to two milliliters of blood were collected in vacutainer tubes at prescribed time points for complete blood cell and pancreatic enzyme panel analysis. Animals were sedated and then euthanized at the end of the study by an intracardiac injection of pentobarbital sodium and phenytoin sodium (Euthasol, MWI Animal Health, USA). All procedures used in this work were reviewed and approved by the Virginia Tech Institutional Animal Care and Use Committee (Protocol #19–117 & #22–022).

2.2. Histotripsy system and pressure calibrations

Histotripsy was performed *in vivo* using a custom 32-element, 500 kHz large animal histotripsy transducer with a geometric focus of 78 mm, an elevational aperture size of 112

Author Manuscript Author Manuscript Author Manuscript Author Manuscript

mm, and a transverse aperture size of 128 mm. The transducer contained two rectangular rings of 14 and 18 20-mm diameter piezoelectric elements arranged around a central hole in the therapy transducer sized to fit a coaxially aligned curvilinear ultrasound imaging probe (Figure 2(A)). Transducer f-numbers were 0.70 and 0.61 in the elevational and transverse directions, respectively. The bubble cloud dimensions in the axial, transverse, and elevational directions were measured to be 5.0 mm, 1.5 mm, and 1.5 mm at a peak negative pressure (p-) of 33 MPa, as previously described [34]. To generate short therapy pulses <2 cycles, the transducer was controlled *via* a custom high-voltage pulser with a field-programmable gate array (FPGA) board (Altera DE0-Nano Terasic Technology, Dover, DE, USA) programmed for histotripsy therapy pulsing [35,36]. The transducer was mounted onto a prototype clinical histotripsy treatment cart (HistoSonics, Ann Arbor, MI, USA) consisting of an ultrasound imaging system, robotic micro-positioner, and customized software designed for applying automated volumetric abla-tions with histotripsy (Figure 2(A)) [27]. A central hole through the therapy transducer allowed a 3 MHz curvilinear imaging probe (Model C5–2, Analogic Corp., Peabody, MA) to be coaxially aligned, enabling real-time treatment guidance and monitoring. During histotripsy treatments, the custom transducer was controlled using a custom user interface operated through MATLAB (MathWorks) and triggered from the HistoSonics' cart software while being powered by a high-voltage DC power supply (GENH750W, TDK-Lambda). The overall setup for the treatment is illustrated in Figure 2.

Focal pressure waveforms for the 500 kHz transducer were collected using a high-sensitivity rod hydrophone (HNR-0500, Onda Corporation, Sunnyvale, CA, USA) and a custom-built fiber optic probe hydrophone (FOPH) [37,38] in degassed water at the focus of the transducer. 1D focal beam profiles of the transducer were measured in the lateral, elevational, and axial directions with the rod hydrophone at a peak negative pressure (p-) of ~1.8 MPa. The FOPH directly measured focal pressures up to a p-limit of ~20 MPa due to cavitation on the tip of the FOPH fiber. Pressure waveforms at higher p- (>20 MPa) were then estimated by the summation of subset measurements from a quarter and a half of the total elements on the transducer as previously described [39]. All waveforms were captured at a sample rate of 500MS/s using a Tektronix TBS2000 series oscilloscope with the waveforms averaged over 128 pulses and recorded in MATLAB. This procedure with further details is described in previous studies [39–41].

2.3. Histotripsy in vivo pancreas ablation procedure

Histotripsy was applied to the porcine pancreas using the custom 500 kHz system described in the previous section, following a treatment workflow previously developed for the treatment of liver cancer [21,25,27,31,42]. Before treatment, freehand ultrasound imaging was performed by a board-certified veterinary radiologist (M.L.) or veterinary radiology resident (M.E.) to identify the pancreas and determine the desired treatment location using either a linear ultrasound imaging probe with a frequency range of 10–18 MHz (L18–10L30H-4, Telemed, Lithuania, EU) or a 3 MHz curvilinear imaging probe (Model C5–2, Analogic Corp., Peabody, MA) (Figure 2(B)). To ensure ultrasound propagation to targeted tissue, a degassed water bolus was coupled to the skin over the pig abdomen using a modified Ioban drape (MMM 6640EZ, 3 M Healthcare, USA) with a central hole to allow

Author Manuscript Author Manuscript Author Manuscript Author Manuscript

ultrasound to be applied directly through an open acoustic window. The surgical drape was attached to a plastic ultrasound-mediated coupling (UMC) bowl that was attached to an articulating arm mounted to the surgical table. The UMC was then filled with degassed water for ultrasound coupling. The therapy transducer with a coaxial imaging probe mounted onto a mechanical arm containing a micro-positioner (Histosonics Inc., Ann Arbor, MI) [27] was then manually positioned to align with the acoustic window identified during freehand imaging (Figure 2(C)).

For treatment, the coaxial imaging probe was used to align the focus of the transducer to the targeted location. Once the focus of the transducer was aligned with the desired region in the pancreas, the therapy transducer was turned on and histotripsy was applied noninvasively using single-cycle pulses and a pulse repetition frequency (PRF) of 500 Hz. The cavitation threshold within the tissue was first determined by slowly increasing the pressure until a robust bubble cloud was generated. A volumetric ablation (0.5–1.8 cm^3) was then applied to the pancreas by sweeping the transducer through a spherical or ellipsoidal ablation volume twice to deliver a total of ~1000 pulses per treatment point. Due to the small size of the pancreas (roughly 1–2cm in height and width seen on coaxial ultrasound imaging), small ablation volumes were targeted in an attempt to keep the ablation lesion fully encapsulated by the pancreatic tissue. Animals were treated at peak negative pressures of ~21–41 MPa. While each subject received the custard laxative, there were variable levels of blockage, and therefore aberration effects, leading to a range of pressures used in an attempt to generate a bubble cloud in all subjects. The *in situ* focal pressures could not be directly measured noninvasively. Using 0.5 dB/cm-MHz attenuation for overlying tissue that was roughly 3 cm overlying the targeted pancreas, the *in situ* peak negative pressures were estimated to be ~19–38 MPa. However, this is likely an overestimate of the actual *in situ* pressure since this estimate does not account for gas blockage attenuation and tissue aberration, which recent work has shown can be significant for intra-abdominal histotripsy procedures [43]. For most subjects, treatment began slightly deeper in the tissue from the cavitation threshold test point to account for a prefocal shift in the bubble cloud location on the US imaging software *in vivo*. Pancreas targeting for all pigs is summarized in Table 1. Throughout the entire procedure, ultrasound imaging was used to monitor the treatment in real-time. After treatment, the therapy transducer was removed, and freehand ultrasound imaging was performed to assess for any tissue damage. Animals in the 1-week group ($n = 4$) were recovered following treatment and survived for 1 week after treatment, as described above. A full necropsy was conducted by a board-certified veterinary pathologist (S.C.O. or K.E.) at the conclusion of the study for all subjects.

2.4. Contrast enhanced computed tomography imaging

Pigs in the second set of experiments underwent an abdominal helical CT evaluation that included non-enhanced and contrast-enhanced triple-phase CT through the abdomen at the time points outlined in Figure 1(B). CT images were acquired with a multi-slice helical CT unit (Aquilion 16, Toshiba Medical Systems Corp., Otawara, Japan). For imaging, each subject was in dorsal recumbency and under sedation for the duration of the CT. The tube rotation speed was 0.5 s, the slice thickness was 2 mm, and the pitch factor was 0.938. All phases of scanning were initiated at the cranial aspect of the diaphragm and

Author Manuscript Author Manuscript Author Manuscript Author Manuscript

extended caudally to the level of the pelvic inlet. Iohexol (300 mg I/mL, Omnipaque 300, GE Healthcare, USA) was used as the contrast medium at a dose of 2.2 ml/kg and was injected with a power injector (Medrad Stellant, Indianola, PA). Scan delay was triggered off the abdominal aorta at the level of the diaphragm for the arterial phase, measuring the mean of Hounsfield units (HU) in the non-enhanced aorta and adding 30HU to determine the HU to trigger the system to begin scanning. The pancreatic phase was scanned immediately after the arterial scan was completed, and the table was translated back to the area of the diaphragm. The equilibrium phase was scanned after 3 min from the time the contrast medium injection started. Images were evaluated by a veterinary radiologist (M.L.) or (M.E.).

2.5. Necropsy & histological analysis

A full necropsy and tissue harvest was performed either immediately or 1-week post-treatment by a board-certified veterinary pathologist (S.C.O. or K.E.) (Figure 1). Gross damage to internal organs was determined with inspection *in situ* and *ex vivo* with serial sections spaced approximately 1 cm apart. Serial slicing of pancreatic tissue was performed after fixation to preserve tissue architecture. Pancreatic tissue and any tissue with noted gross changes were visually inspected and fixed in 10% formalin for at least 24 h before sectioning, embedding, and staining. All tissues were stained using hematoxylin and eosin (H&E) to assess for histotripsy damage. Additionally, any other changes in the structure and density of collagen and other tissue structures (i.e. vasculature and bile ducts) within the ablation volume were also noted. Analysis was led by veterinary pathologists to ensure accuracy and avoid biases.

3. Results

3.1. Study 1: Histotripsy targeting and ablation of pancreas – fasted pigs

In the initial pilot study of 3 pigs fasted for 12 h prior to treatment (Figure 1(A)), ultrasound imaging showed significant amounts of gas in the stomach and intestines overlying the pancreas, limiting the ability to precisely apply histotripsy to the pancreas (Figure 3). On freehand ultrasound imaging in these animals, the pancreas body could only be visualized when significant pressure was placed on the abdomen with the imaging probe in order to push the overlying gas-filled tissues out of the imaging path (Figure 3(A)). Once the histotripsy transducer was placed over the subject, the pancreas was completely obscured by the overlying gas-containing tissues (Figure 3(B)). In all 3 subjects in the pilot study, the pancreas could not be visualized with the imaging probe inside of the therapy transducer, which prevented histotripsy from being applied to the pancreas precisely with real-time imaging feedback. Although the pancreas could not be directly visualized in these animals, histotripsy treatments were still applied after aligning the focus of the transducer as closely as possible to the anatomical region expected to contain the pancreas. Results from treatments showed cavitation damage in regions near the transducer focus as well as in pre-focal regions outside of the focus (Figure 3(C and D)). After treatment, ultrasound imaging results showed no clear signs of a histotripsy lesion generated in the pancreas on freehand ultrasound imaging, nor was there any sign of damage outside of the targeted region. During the necropsy of all 3 pigs, clear signs of histotripsy-induced cavitation

Author Manuscript Author Manuscript Author Manuscript Author Manuscript

damage were observed in multiple locations in tissues overlying the pancreas (Figure 3(C and D)), with no signs of treatment-related changes occurring within the pancreas. The damage shown in Figure 3 is representative of all 3 pigs. For instance, Figures 3(C and D)) show intestinal bruising in the region above the pancreas, with the extent of the intestinal bruising more highly concentrated in the large intestine. Post-treatment H&E histopathology of these regions showed significant damage to the submucosal regions of the bruised colon (Figure 3(E and F)). However, the muscularis regions of the colon were not ruptured (Figure 3(E and F)), with this trend consistent for all regions of the intestines that showed bruising during necropsy for all 3 pigs.

3.2. Study 2: Histotripsy targeting and ablation of pancreas – specialty diet pigs

In the second part of this study, ultrasound imaging and necropsy results (Figure 4, 5, 6, and 7) showed improvements in the visualization of the pancreas in these subjects in comparison to the pigs in the pilot study (Figure 3), suggesting that the speciality diet (SD) reduced the gas content inside of the stomach and intestines in the acoustic window overlying the pancreas. On freehand ultrasound imaging, regions of the pancreas (head, tail, and body) were clearly visualized using minimal pressure applied to the imaging probe with the pancreas tail being the most identified in 5 out of the 8 SD pigs (Table 1). Figure 4(A) and Figure 5(A) are representative of the pancreas visualization on freehand ultrasound imaging for the acute and chronic SD pigs, respectively. When the histotripsy transducer was placed over the subject, the same regions of the pancreas seen on freehand ultrasound were mostly visualized on the coaxial imaging probe in 50% of the SD pigs (Table 1). Previous histotripsy studies have shown that the imaging quality significantly degrades when switched to the coaxial US imaging probe due to the required stand-off and this degradation may have been exacerbated by the ability to apply significant pressure with the freehand imaging probe to dislodge the overlying bowel. Figure 4(B) and Figure 5(B) are representative of the coaxial ultrasound visualization of the pancreas for the acute and chronic SD pigs, respectively. Results from the histotripsy treatments showed well-defined cavitation bubble clouds formed at the focus of the transducer in 50% of the SD pigs. Figure 4(C) and Figure 5(C) show the dynamically changing hyperechoic bubble cloud on ultrasound imaging for a given treatment. During the histotripsy treatment, small amounts of pre-focal cavitation were observed in Pigs SD-2, SD-4, and SD-6 on ultrasound imaging. Immediately after treatment, ultrasound imaging results did not show a hypoechoic region to indicate ablation for most pigs (Figure 4(D)), likely due to limitations in imaging quality and the small ablation zones treated in this pilot study. However, after histotripsy treatment of Pig SD-5, a clear hypoechoic region was observed on ultrasound imaging identifying the targeted ablation volume (Figure 5(D)). This observation was only seen in this pig, suggesting there was a definitive histotripsy treatment only in Pig SD-5.

During necropsy for the acute group ($n = 4$), there was no off-target damage observed by the pathologist in Pigs SD-1, SD-2, and SD-3 (Figure 6(A and B)). Necropsy of Pig SD-4 revealed minor bruising on the bowel that was more concentrated compared to the pilot group (Figure 6(C)). Post-treatment H&E histopathology revealed notable lesions on the intestines that had a loss of tissue structure indicating off-target damage. Post-treatment H&E histopathology also revealed no significant necrosis in the pancreas

Author Manuscript Author Manuscript Author Manuscript Author Manuscript

in these pigs (Figure 6(D)). After 1 week post-treatment, gross morphology showed no off-target damage in overlying organs in Pig SD-5 during necropsy, despite the noted pre-focal cavitation during treatment (Figure 7(A–E)). At the conclusion of the 1-week survival study, gross necropsies were performed on each animal to evaluate for treatment-related effects. Gross examination of the liver, pancreas, spleen, gastrointestinal tract, and kidneys was unremarkable. No evidence of inflammation, hemorrhage, perforation, or other pathology was identified. There was no splenomegaly, and bread slices to the liver and spleen further confirmed no off-target ablation within those organs. Bread slices of formalin-fixed pancreas tissues did not reveal any gross lesions. Histology from the 1-week necropsy showed no notable lesions, hemorrhage, or inflammation within the pancreas (Figure 7(F)). CT showed that there was no free fluid in the abdomen (Figure 7(G)). In pigs that underwent CT, the pancreas exhibited mild diffuse homogeneous contrast enhancement, with smooth regular margins. No evidence of a lesion is present on the CT exams or off-target damage, suggesting that the treatments were well-tolerated even in cases where therapy was applied using anatomical alignment rather than direct visualization of the pancreas during therapy.

3.3. Clinical outcomes during and after histotripsy pancreas ablation

For all histotripsy procedures conducted in both sets of experiments in this study, the animals tolerated the procedure without physiologic indication of stress. The vital signs of all the pigs showed no negative responses to treatment. For instance, during and after the histotripsy treatment, the heart rate and respiration rates were both maintained within ±5% of the baseline values observed before treatment. Similarly, blood oxygen levels showed that the SpO_2 remained above 95% for the duration of the procedure, and core body temperature was maintained between ~32 and 39 °C. After treatment, all animals in the 1 week-survival group ($n = 4$) were awakened from anesthesia without any signs of distress or discomfort. All animals recovered well from treatment and were returned to standard housing with their normal, unrestricted diet within 4 h of treatment. Over the week following treatment, the animals had no signs of debilitating side effects, distress, or discomfort. Specifically, there was no note of fatigue, pain, vomiting, diarrhea or discolored stool in any of the animals. All animals maintained normal weight, eating and drinking habits, levels of activity, and socialization. No abnormalities were noted on the complete blood cell or blood chemistry panels. Analysis of blood samples for the 4 chronic SD pigs showed average WBC levels of $19.87 \pm 10.29 \times 10^3$ cells/μL, $17.75 \pm 2.76 \times 10^3$ cells/μL, and $29.05 \pm 10.60 \times 10^3$ cells/μL [reference range, $10–25 \times 10^3$ cells/μL] for baseline, 1-day post-treatment, and 5-days post-treatment levels, respectively. The average WBC level 5-days post-treatment was the only group above the reference ranges due to one of the pig's WBC levels being elevated at the 5-days post-treatment mark. This same pig also had elevated baseline WBC levels compared to the other pigs before histotripsy treatment. Even though this pig exhibited elevated WBC levels before and after therapy, these levels are not high enough to be indicative of pancreatitis. For reference, a recent study that developed an acute pancreatitis porcine model showed serum amylase and lipase levels being at least three times greater than the baseline values at all post-procedural time points in all pigs [44]. These results agree with what is seen clinically with pancreatitis in human patients with serum levels being elevated 2–4 times that of baseline [45]. Average amylase levels were 993.25 ± 447.45 U/L, 770.67 ± 171.34 U/L, and 1109 ± 388.77 U/L [reference range, 650–4500 U/L] for baseline, 1-day

Author Manuscript Author Manuscript Author Manuscript Author Manuscript

post-treatment, and 5-days post-treatment levels, respectively. Average lipase levels were 11.58 ± 5.70 U/L, 6.97 ± 4.17 U/L, 7.05 ± 4.00 U/L [Duchess Fund reference range, 0–200 U/L] for baseline, 1-day post-treatment, and 5 days post-treatment levels, respectively. Note that 1-day post-treatment was unable to be collected for one pig. Levels of all animals were not significantly affected by histotripsy treatment when measured 1 and 5-days after treatment compared to their baseline values determined 5-days prior to treatment. Reference levels were obtained from the Virginia Maryland College of Veterinary Medicine Virginia Tech Animal Laboratory Services (ViTALS).

4. Discussion

In this study, we investigated the feasibility of using histotripsy for pancreatic tissue ablation in an *in vivo* porcine model. The noninvasive nature of histotripsy minimizes the risks of infection that are present with more invasive techniques. Ultrasound targeting of intra-abdominal organs such as the pancreas, requires careful planning and investigation to determine the ideal preoperative and operative procedures in order to minimize the effects of pre-focal cavitation and to avoid gas within the gastrointestinal tract which limits visualization. Given that two of the notable benefits of histotripsy as an ablation modality are that it is noninvasive and ultrasound image-guided, the focus of this study was to determine the feasibility of this approach to targeting the pancreas. A prior porcine study utilizing HIFU to treat the pancreas was able to perform the procedure using a laxative-laced custard diet without the use of a nasogastric tube or other invasive techniques to remove the gas from the gastrointestinal tract [32], which could also be explored for histotripsy in future studies. In this study, a combination of simethicone, laxative, and custard, previously reported as noninvasive methods for degassing the stomach and intestines [32,33], was used to help improve acoustic access to healthy pig pancreas. Results demonstrated that this speciality diet improved acoustic access to the pancreas, allowing histotripsy to be applied to the pancreas in 50% of the subjects. It is expected that additional refinements to this dietary protocol and the implementation of other strategies to remove the gas in overlying tissues will allow for improved ultrasound visualization of the pancreas in a larger percentage of subjects. For instance, additional studies could explore the use of activated charcoal in addition to simethicone to reduce gastrointestinal gas, which has already been shown to improve ultrasound visualization of the pancreas in humans [46]. Moreover, future studies should also explore the use of more advanced targeting and monitoring methods that are in development for other applications such as image-fusion and 3D passive cavitation mapping [47–49]. These tools may ultimately be needed to safely apply histotripsy in a larger percentage of pancreatic cancer patients. Finally, histological results from this study did not identify clear regions of ablation within the pancreas as were seen on US imaging. This discrepancy could be due to the small volumes (0.5–1.8 cm^3) used in this study making it extremely difficult for the pathologist to section the treated tissue, especially since there was no hemorrhagic region on the pancreas upon necropsy to identify the ablation zone. For the chronic pig where a hypoechoic ablation zone was visualized on US imaging, the small lesion could have resolved over the course of 1-week suggesting that histotripsy pancreas treatments are well-tolerated and do not induce pancreatitis. However, a goal in our future work is to obtain histological data showing larger histotripsy-treated lesions in

Author Manuscript Author Manuscript Author Manuscript Author Manuscript

the pancreas and/or pancreatic tumors in a larger number of subjects to demonstrate the therapy's precision as prior studies have shown in the liver and other organs.

While this pilot study using histotripsy to target the pancreas was preliminary, the safety profile showed promising results that suggest histotripsy should be further explored for the treatment of pancreatic cancer. Although a clinical histotripsy treatment would require prior visualization of the pancreas to deliver therapy, histotripsy was still applied to all pigs in this study in order to assess the safety profile in a worst-case scenario. These cases showed that histotripsy treatment was still well-tolerated during the procedure while highlighting the potential off-target damage that can occur without proper treatment guidance and monitoring techniques. These off-target effects are a significant hurdle for non-invasive ablation techniques like histotripsy, particularly for structures like the pancreas which are surrounded by critical structures. Results from this study suggest that histotripsy could be used to effectively target the pancreas without causing damage to nearby critical structures in cases where the pancreas and histotripsy bubble cloud could be properly visualized on ultrasound imaging. This is a requirement for all clinical histotripsy treatments and represents the most clinically relevant results of this study as the therapy would not be delivered in a clinical setting without confirmation of target visualization. However, for the purposes of this exploratory pilot study, histotripsy was also delivered to the pancreas using anatomical alignment in cases in which the pancreas was not clearly visualized prior to treatment. In these cases, the procedures were still well-tolerated with no significant adverse events noted during therapy. While off-target intestinal bruising was identified, there were no signs of pancreatitis, intestinal perforation, intraabdominal bleeding, or pancreatic fistulas. It is again important to note that some of the procedures performed in this pilot study would not be conducted in a clinical setting, which would require direct visualization of the targeted tissue prior to applying histotripsy and throughout the procedure. To mitigate unwanted side effects due to mis-targeting, it is important for clinicians to be able to clearly visualize the targeted pancreatic region with ultrasound or other imaging modalities prior to histotripsy treatment as well as monitor the focal bubble cloud within the pancreas during treatment. Therefore, the results of this study show that it is imperative that a consistent patient preparation regimen is implemented to eliminate overlying gastrointestinal gas. While the speciality diet proved more effective than fasting in this study, future work is needed to improve pancreas visualization more consistently on ultrasound. In addition, supplemental studies should explore the potential for cavitation generation in prefocal tissues overlying the pancreas, which was observed in some of these treatments, particularly those with limited visualization of the pancreas on ultrasound imaging. Although it is expected that prefocal cavitation will be less of an issue when targeting pancreatic tumors, which are much larger than the healthy pancreas regions targeted in this study, understanding the risk of pre-focal cavitation and developing proper mitigation strategies will be essential to advancing histotripsy for this application.

In addition to evaluating any off-target damage caused by histotripsy, the results of this study also reported no signs of pancreatitis, which is a concern that has been previously reported in association with other ablation modalities [50,51]. Determining if an ablation therapy causes pancreatitis is important due to the ability to treat margins without causing negative side effects. Given that the porcine pancreas is similar in anatomy and presentation

Author Manuscript Author Manuscript Author Manuscript Author Manuscript

of acute pancreatitis to humans [52–54], they make an appropriate model for investigating histotripsy's safety profile. A previous porcine study testing the use of IRE within the pancreas showed a rise in WBCs, amylase, and lipase as well as anorexia after treatment [55]. These findings were not noted in any of the 4 chronic pigs in our study, providing promising initial evidence that histotripsy can be well-tolerated in the pancreas. For reference, a recent study that developed an acute pancreatitis porcine model showed serum amylase and lipase levels being at least three times greater than the baseline values at all post-procedural time points in all pigs [44]. These results agree with what is seen clinically with pancreatitis in human patients with serum levels being elevated 2–4 times that of baseline [45]. Although some of the serum levels in this study were elevated from baseline, none of the post-histotripsy treatment levels were elevated by three times as much as the baseline value indicative of acute pancreatitis. Furthermore, the subjects were clinically asymptomatic with the transient elevation in serum enzymes. Similarly, the results of this pilot study did not note any signs of pancreatic fistula formation, which is an additional concern for histotripsy. By histotripsy being non-thermal, there is increased concern about fistula formation due to the mechanical breakdown of the tissue. The 2016 International Study Group of Pancreatic Fistula redefined a pancreatic fistula as post-operative drainage from the pancreas that results in a Sequelae that requires clinical intervention to prevent mortality [56,57]. From the 4 pigs that survived for 1 week after histotripsy in this study, there were no changes to behavior or diet and no signs on CT or necropsy to indicate that a pancreatic fistula was formed. One reason for this could be due to the collagenous nature of the pancreatic duct which resists the mechanical destruction secondary to the intrinsic tissue properties. However, further studies on this must be done in order to understand this phenomenon, as preservation of the pancreatic duct will be critical for the clinical translation of histotripsy in pancreatic cancer.

Although the general findings of this study were positive and suggest that additional studies should be pursued to develop histotripsy for the treatment of pancreatic cancer, there were many notable limitations to this pilot study in addition to those listed above. First, this study was only conducted on a small number of animals, with the treatment effects only monitored for a maximum of 1 week after treatment. Additional studies are warranted to investigate the long-term safety of histotripsy in a larger number of animals with longer follow-up times to provide more compelling data establishing the safety of histotripsy in the pancreas. A second limitation of this study was the treatment of healthy pancreas in all subjects, which does not replicate the clinical case of treating pancreatic tumors. While previous studies have shown that stiffer tissues are less susceptible to histotripsy [23], recent work by our team and others has demonstrated the effective breakdown of more fibrous tissue types at higher treatment doses. For instance, a single-cycle histotripsy pulsing regime was used to break down uterine fibroids [58] and multi-cycle shock-scattering histotripsy effectively broke down cholangiocarcinoma liver tumors [59]. This work also aligns with other work demonstrating boiling histotripsy's ability to break down fibrotic prostate tissue [60]. Additionally, these studies showed that single-cycle intrinsic threshold histotripsy performed better than the 5-cycle shock-scattering regime due to the formation of a denser nucleated bubble cloud. Future studies are planned to address this limitation by testing histotripsy for pancreatic cancer ablation in our recently developed immunocompromised

Author Manuscript Author Manuscript Author Manuscript Author Manuscript

pigs with implanted human pancreatic tumors [61]. From these studies, we expect multiple histotripsy regimes will be able to be effectively utilized for the breakdown of pancreatic tumors. Future work should investigate the optimization of histotripsy pulsing schemes for fibrous tissue ablation. Together, these studies will aid in the clinical translation of histotripsy for pancreatic cancer by understanding the safety profile and limitations of the modality for improved development.

5. Conclusion

This proof-of-concept study demonstrates the feasibility of histotripsy for the noninvasive ablation of the pancreas in a porcine model for the first time. Results from this study provides initial evidence suggesting that histotripsy can be used to safely target and treat the pancreas without inducing significant side effects of pancreatitis. This study also highlights the challenges of ultrasound-guidance for histotripsy of the pancreas and the need for improved strategies to reduce intestinal gas prior to treatment in order to allow for histotripsy to be applied using ultrasound-guided methods. Overall, this study suggests that future work is warranted to explore histotripsy for pancreas ablation and evaluate the potential of histotripsy as a new method for the noninvasive ablation of pancreatic tumors.

Supplementary Material

Refer to Web version on PubMed Central for supplementary material.

Acknowledgements

The content is solely the responsibility of the authors and does not necessarily represent the official views of the NIH or any other funding agency. The authors would like to thank HistoSonics, Inc. for providing the clinical histotripsy cart for this study. This article includes research previously included in a thesis entitled “Determining the Oncological and Immunological Effects of Histotripsy for Tumor Ablation” authored by Alissa Hendricks-Wenger.

Funding

This work was supported by the Virginia Maryland College of Veterinary Medicine; The Virginia Tech Institute for Critical Technology and Applied Sciences Center for Engineered Health; The National Institutes of Health (EB028429, CA269811); and the Focused Ultrasound Foundation (FUF61057). Author Jessica Gannon was supported by a National Science Foundation Graduate Research Fellowship for the duration of this work.

Data availability statement

The data presented in this study are available on request from the corresponding authors.

References

[1]. Siegel RL, Miller KD, Jemal A. Cancer statistics, 2020. CA Cancer J Clin. 2020;70(1):7–30. doi: 10.3322/caac.21590. [PubMed: 31912902]

[2]. Mizrahi JD, Surana R, Valle JW, et al. Pancreatic cancer. Lancet. 2020;395(10242):2008–2020. doi: 10.1016/S0140-6736(20)30974-0. [PubMed: 32593337]

[3]. Chiorean EG, Coveler AL. Pancreatic cancer: optimizing treatment options, new, and emerging targeted therapies. Drug Des Devel Ther. 2015;9:3529–3545. doi: 10.2147/DDDT.S60328.

[4]. Artinyan A, Soriano PA, Prendergast C, et al. The anatomic location of pancreatic cancer is a prognostic factor for survival. HPB. 2008;10(5):371–376. doi: 10.1080/13651820802291233. [PubMed: 18982154]

Author Manuscript Author Manuscript Author Manuscript Author Manuscript

[5]. Paiella S, Malleo G, Cataldo I, et al. Radiofrequency ablation for locally advanced pancreatic cancer: SMAD4 analysis segregates a responsive subgroup of patients. Langenbecks Arch Surg. 2018;403(2):213–220. doi: 10.1007/s00423-017-1627-0. [PubMed: 28983662]

[6]. Ge H-Y, Miao L-Y, Xiong L-L, et al. High-intensity focused ultrasound treatment of late-stage pancreatic body carcinoma: optimal tumor depth for safe ablation. Ultrasound Med Biol. 2014;40(5):947–955. doi: 10.1016/j.ultrasmedbio.2013.11.020. [PubMed: 24462161]

[7]. Keisari Y Tumor abolition and antitumor immunostimulation by physico-chemical tumor ablation. Front Biosci. 2017;22(2):310–347. doi: 10.2741/4487.

[8]. Sofuni A, Moriyasu F, Sano T, et al. Safety trial of high-intensity focused ultrasound therapy for pancreatic cancer. World J Gastroenterol. 2014;20(28):9570–9577. doi: 10.3748/wjg.v20.i28.9570. [PubMed: 25071354]

[9]. Sugimoto K, Moriyasu F, Tsuchiya T, et al. Irreversible electroporation for nonthermal tumor ablation in patients with locally advanced pancreatic cancer: initial clinical experience in Japan. Intern Med. 2018;57(22):3225–3231. doi: 10.2169/internalmedicine.0861-18. [PubMed: 29984761]

[10]. Ierardi AM, et al. Percutaneous ablation therapies of inoperable pancreatic cancer: a systematic review. Ann Gastroenterol. 2015;28(4):431–439. [PubMed: 26424487]

[11]. D'Onofrio M, Ciaravino V, De Robertis R, et al. Percutaneous ablation of pancreatic cancer. World J Gastroenterol. 2016;22(44):9661–9673. doi: 10.3748/wjg.v22.i44.9661. [PubMed: 27956791]

[12]. Vidal-Jove J, Perich E, Del Castillo MA. Ultrasound guided high intensity focused ultrasound for malignant tumors: the spanish experience of survival advantage in stage III and IV pancreatic cancer. Ultrason Sonochem. 2015;27:703–706. doi: 10.1016/j.ultsonch.2015.05.026. [PubMed: 26044461]

[13]. Mouratidis PXE, Ter Haar G. Latest advances in the use of therapeutic focused ultrasound in the treatment of pancreatic cancer. Cancers. 2022;14(3, p):638. doi: 10.3390/cancers14030638. [PubMed: 35158903]

[14]. Timmer FEF, Geboers B, Ruarus AH, et al. Irreversible electroporation for locally advanced pancreatic cancer. Tech Vasc Interv Radiol. 2020;23(2):100675. // doi: 10.1016/j.tvir.2020.100675. [PubMed: 32591191]

[15]. Linecker M, Pfammatter T, Kambakamba P, et al. Ablation strategies for locally advanced pancreatic cancer. Dig Surg. 2016; 33(4):351–359. doi: 10.1159/000445021. [PubMed: 27216160]

[16]. Vlaisavljevich E, Maxwell A, Mancia L, et al. Visualizing the histotripsy process: bubble Cloud-Cancer cell interactions in a tissue-mimicking environment. Ultrasound Med Biol. 2016;42(10):2466–2477. doi: 10.1016/j.ultrasmedbio.2016.05.018. [PubMed: 27401956]

[17]. Xu Z, Ludomirsky A, Eun LY, et al. Controlled ultrasound tissue erosion. IEEE Trans Ultrason Ferroelectr Freq Control. 2004;51(6):726–736. doi: 10.1109/tuffc.2004.1308731. [PubMed: 15244286]

[18]. Xu Z, Raghavan M, Hall TL, et al. Evolution of bubble clouds induced by pulsed cavitational ultrasound therapy - histotripsy. IEEE Trans Ultrason Ferroelectr Freq Control. 2008;55(5):1122–1132. doi: 10.1109/TUFFC.2008.764. [PubMed: 18519220]

[19]. Vlaisavljevich E, Lin K-W, Warnez MT, et al. Effects of tissue stiffness, ultrasound frequency, and pressure on histotripsy-induced cavitation bubble behavior. Phys Med Biol. 2015;60(6):2271–2292. doi: 10.1088/0031-9155/60/6/2271. [PubMed: 25715732]

[20]. Mancia L, Vlaisavljevich E, Xu Z, et al. Predicting tissue susceptibility to mechanical cavitation damage in therapeutic ultrasound. Ultrasound Med Biol. 2017;43(7):1421–1440. doi: 10.1016/j.ultrasmedbio.2017.02.020. [PubMed: 28408061]

[21]. Vlaisavljevich E, Owens G, Lundt J, et al. Non-Invasive liver ablation using histotripsy: preclinical safety study in an in vivo porcine model. Ultrasound Med Biol. 2017;43(6):1237–1251. doi: 10.1016/j.ultrasmedbio.2017.01.016. [PubMed: 28318889]

[22]. Kim Y, Vlaisavljevich E, Owens GE, et al. In vivo transcostal histotripsy therapy without aberration correction. Phys Med Biol. 2014;59(11):2553–2568. doi: 10.1088/0031-9155/59/11/2553. [PubMed: 24785433]

Author Manuscript Author Manuscript Author Manuscript Author Manuscript

[23]. Vlaisavljevich E, Kim Y, Owens G, et al. Effects of tissue mechanical properties on susceptibility to histotripsy-induced tissue damage. Phys Med Biol. 2014;59(2):253–270. doi: 10.1088/0031-9155/59/2/253. [PubMed: 24351722]

[24]. Lake AM, Xu Z, Wilkinson JE, et al. Renal ablation by histotripsy– does it spare the collecting system? J Urol. 2008;179(3):1150–1154. doi: 10.1016/j.juro.2007.10.033. [PubMed: 18206166]

[25]. Vlaisavljevich E, Kim Y, Allen S, et al. Image-Guided Non-Invasive ultrasound liver ablation using histotripsy: feasibility study in an in vivo porcine model. Ultrasound Med Biol. 2013;39(8):1398–1409. doi: 10.1016/j.ultrasmedbio.2013.02.005. [PubMed: 23683406]

[26]. Mancia L, Vlaisavljevich E, Yousefi N, et al. Modeling tissue-selective cavitation damage. Phys Med Biol. 2019;64(22):225001. doi: 10.1088/1361-6560/ab5010. [PubMed: 31639778]

[27]. Smolock AR, Cristescu MM, Vlaisavljevich E, et al. Robotically assisted sonic therapy as a noninvasive nonthermal ablation modality: proof of concept in a porcine liver model. Radiology. 2018;287(2):485–493. doi: 10.1148/radiol.2018171544. [PubMed: 29381870]

[28]. Wang TY, Hall TL, Xu Z, et al. Imaging feedback of histotripsy treatments using ultrasound shear wave elastography. IEEE Trans. Ultrason., Ferroelect., Freq. Contr. 2012;59(6):1167–1181. doi: 10.1109/TUFFC.2012.2307.

[29]. Lundt JE, Allen SP, Shi J, et al. Non-invasive, rapid ablation of tissue volume using histotripsy. Ultrasound Med Biol. 2017;43(12):2834–2847. doi: 10.1016/j.ultrasmedbio.2017.08.006. [PubMed: 28935135]

[30]. Xu Z, Hall TL, Vlaisavljevich E, et al. Histotripsy: the first noninvasive, non-ionizing, non-thermal ablation technique based on ultrasound. Int J Hyperthermia. 2021;38(1):561–575. doi: 10.1080/02656736.2021.1905189. [PubMed: 33827375]

[31]. Vidal-Jove J, Serres X, Vlaisavljevich E, et al. First-in-man histotripsy of hepatic tumors: the THERESA trial, a feasibility study. Int J Hyperthermia. 2022;39(1):1115–1123. doi: 10.1080/02656736.2022.2112309. [PubMed: 36002243]

[32]. Sebeke LC, Rademann P, Maul AC, et al. Feasibility study of MR-guided pancreas ablation using high-intensity focused ultrasound in a healthy swine model. Int J Hyperthermia. 2020;37(1):786–798. doi: 10.1080/02656736.2020.1782999. [PubMed: 32619373]

[33]. Ge H-Y, Miao L-Y, Wang J-R, et al. Correlation between ultrasound reflection intensity and tumor ablation ratio of late-stage pancreatic carcinoma in HIFU therapy: dynamic observation on ultrasound reflection intensity. ScientificWorldJournal. 2013;2013:852874. doi: 10.1155/2013/852874. [PubMed: 24453916]

[34]. Hendricks-Wenger A, Arnold L, Gannon J, et al. Histotripsy ablation in preclinical animal models of cancer and spontaneous tumors in veterinary patients: a review. IEEE Trans Ultrason Ferroelectr Freq Control. 2022;69(1):5–26. doi: 10.1109/tuffc.2021.3110083. [PubMed: 34478363]

[35]. Vlaisavljevich E, Lin K-W, Maxwell A, et al. Effects of ultrasound frequency and tissue stiffness on the histotripsy intrinsic threshold for cavitation. Ultrasound Med Biol. 2015;41(6):1651–1667. doi: 10.1016/j.ultrasmedbio.2015.01.028. [PubMed: 25766571]

[36]. Lin K-W, Kim Y, Maxwell AD, et al. Histotripsy beyond the intrinsic cavitation threshold using very short ultrasound pulses: microtripsy. IEEE Trans Ultrason Ferroelectr Freq Control. 2014;61(2):251–265. doi: 10.1109/TUFFC.2014.6722611. [PubMed: 24474132]

[37]. Parsons JE, Cain CA, Abrams GD, et al. Pulsed cavitational ultrasound therapy for controlled tissue homogenization. Ultrasound Med Biol. 2006;32(1):115–129. doi: 10.1016/j.ultrasmedbio.2005.09.005. [PubMed: 16364803]

[38]. Parsons JE, Cain CA, Fowlkes JB. Cost-effective assembly of a basic fiber-optic hydrophone for measurement of high-amplitude therapeutic ultrasound fields. J Acoust Soc Am. 2006;119(3):1432–1440. doi: 10.1121/1.2166708. [PubMed: 16583887]

[39]. Vlaisavljevich E, Gerhardson T, Hall T, et al. Effects of f-number on the histotripsy intrinsic threshold and cavitation bubble cloud behavior. Phys Med Biol. 2017;62(4):1269–1290. doi: 10.1088/1361-6560/aa54c7. [PubMed: 27995900]

[40]. Holmes HR, Haywood M, Hutchison R, et al. Focused ultrasound extraction (FUSE) for the rapid extraction of DNA from tissue matrices. Methods Ecol. Evol. 2020;11(12):1599–1608. doi: 10.1111/2041-210X.13505.

Author Manuscript Author Manuscript Author Manuscript Author Manuscript

[41]. Khirallah J, Schmieley R, Demirel E, et al. Nanoparticle-mediated histotripsy (NMH) using perfluorohexane ‘nanocones. Phys Med Biol. 2019;64(12):125018. doi: 10.1088/1361-6560/ab207e. [PubMed: 31071701]

[42]. Vidal Jove J, et al. Phase I study of safety and efficacy of hepatic histotripsy. Preliminary results of first in man experience with Robotically-Assisted sonic therapy. Proceedings of the International Society of Therapeutic Ultrasound. Barcelona, Spain, 2019. p. 167.

[43]. Yeats E, Gupta D, Xu Z, et al. Effects of phase aberration on transabdominal focusing for a large aperture, low f-number histotripsy transducer. Phys Me. Biol. 2022;67(15):155004. doi: 10.1088/1361-6560/ac7d90.

[44]. Park JS, Jeong S, Kim JM, et al. Development of an acute pancreatitis porcine model based on endoscopic retrograde infusion of contrast medium or sodium taurocholate, (in eng. Korean J Intern Med. 2019;34(6):1244–1251. doi: 10.3904/kjim.2017.367. [PubMed: 30428647]

[45]. Basnayake C, Ratnam D. Blood tests for acute pancreatitis, (in eng. Aust Prescr. 2015;38(4):128–130. doi: 10.18773/austprescr.2015.043.

[46]. Abdul Jabar A, Abbas I, Mishah N, et al. Effect of adding a capsule with activated charcoal to abdominal ultrasound preparation on image quality. J Ultrason. 2020;20(80):e12–e17. doi: 10.15557/jou.2020.0003. [PubMed: 32320165]

[47]. Wagner MG, Periyasamy S, Kutlu AZ, et al. An X-ray C-arm guided automatic targeting system for histotripsy. IEEE Trans. Biomed. Eng. 2023;70(2):592–602. doi: 10.1109/TBME.2022.3198600. [PubMed: 35984807]

[48]. Mauri G, Cova L, De Beni S, et al. Real-time US-CT/MRI image fusion for guidance of thermal ablation of liver tumors undetectable with US: results in 295 cases, (in eng. Cardiovasc Intervent Radiol. 2015;38(1):143–151. doi: 10.1007/s00270-014-0897-y.

[49]. Sukovich JR, Macoskey JJ, Lundt JE, et al. Real-time transcranial histotripsy treatment localization and mapping using acoustic cavitation emission feedback. IEEE Trans Ultrason Ferroelectr Freq Control. 2020;67(6):1178–1191. doi: 10.1109/TUFFC.2020.2967586. [PubMed: 31976885]

[50]. Ruarus A, Vroomen L, Puijk R, et al. Locally advanced pancreatic cancer: a review of local ablative therapies. Cancers. 2018; 10(1): 16. doi: 10.3390/cancers10010016. [PubMed: 29320420]

[51]. Granata V, Grassi R, Fusco R, et al. Assessment of ablation therapy in pancreatic cancer: the radiologist’s challenge. Front Oncol. 2020;10:560952. doi: 10.3389/fonc.2020.560952. [PubMed: 33330028]

[52]. Ke L, Tong Z-h, Ni H-B, et al. The effect of intra-abdominal hypertension incorporating severe acute pancreatitis in a porcine model. PLoS One. 2012;7(3):e33125. doi: 10.1371/journal.pone.0033125. [PubMed: 22403734]

[53]. Otto J, Afify M, Jautz U, et al. Histomorphologic and ultrastructural lesions of the pancreas in a porcine model of intra-abdominal hypertension. Shock. 2010;33(6):639–645. doi: 10.1097/SHK.0b013e3181cb8be0. [PubMed: 19940813]

[54]. Marchetti P, Finke EH, Gerasimidi-Vazeou A, et al. Automated large-scale isolation, in vitro function and xenotransplantation of porcine islets of langerhans. Transplantation. 1991;52(2):209–213. doi: 10.1097/00007890-199108000-00005. [PubMed: 1871791]

[55]. Bower M, Sherwood L, Li Y, et al. Irreversible electroporation of the pancreas: definitive local therapy without systemic effects. J Surg Oncol. 2011;104(1):22–28. doi: 10.1002/jso.21899. [PubMed: 21360714]

[56]. Nahm CB, Connor SJ, Samra JS, et al. Postoperative pancreatic fistula: a review of traditional and emerging concepts. Clin Exp Gastroenterol. 2018;11:105–118. doi: 10.2147/CEG.S120217. [PubMed: 29588609]

[57]. Bassi C, Marchegiani G, Dervenis C, et al. The 2016 update of the international study group (ISGPS) definition and grading of post-operative pancreatic fistula: 11 years after, (in eng. Surgery. 2017;161(3):584–591. doi: 10.1016/j.surg.2016.11.014. [PubMed: 28040257]

[58]. Simon A, Robinson F, Anzivino A, et al. Histotripsy for the treatment of uterine leiomyomas: a feasibility study in ex vivo uterine fibroids, (in eng. Ultrasound Med Biol. 2022;48(8):1652–1662. doi: 10.1016/j.ultrasmedbio.2022.04.214. [PubMed: 35641394]

Author Manuscript Author Manuscript Author Manuscript Author Manuscript

[59]. Hendricks-Wenger A, Weber P, Simon A, et al. Histotripsy for the treatment of cholangiocarcinoma liver tumors: *in vivo* feasibility and ex vivo dosimetry study. IEEE Trans Ultrason Ferroelectr Freq Control. 2021;68(9):2953–2964. doi: 10.1109/TUFFC.2021.3073563. [PubMed: 33856990]

[60]. Khokhlova VA, Rosnitskiy PB, Tsysar SA, et al. Initial assessment of boiling histotripsy for mechanical ablation of ex vivo human prostate tissue. Ultrasound Med Biol. 2023;49(1):62–71. doi: 10.1016/j.ultrasmedbio.2022.07.014. [PubMed: 36207225]

[61]. Hendricks-Wenger A, Aycock KN, Nagai-Singer MA, et al. Establishing an immunocompromised porcine model of human cancer for novel therapy development with pancreatic adenocarcinoma and irreversible electroporation. Sci Rep. 2021;11(1):7584. doi: 10.1038/s41598-021-87228-5. [PubMed: 33828203]

Author Manuscript Author Manuscript Author Manuscript Author Manuscript

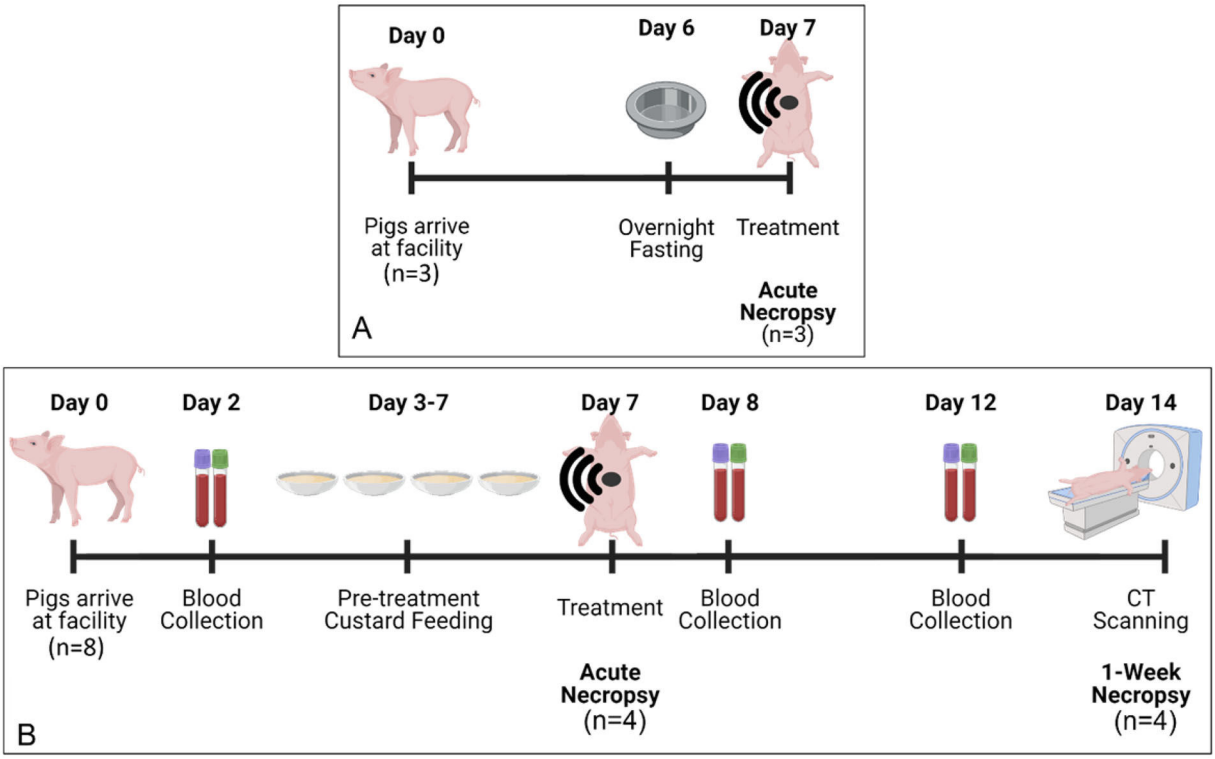


Figure 1.
Timeline. Timeline of first pig study (A). Timeline of second pig study using specialty diet during pig preparation (B).

Author Manuscript Author Manuscript Author Manuscript Author Manuscript

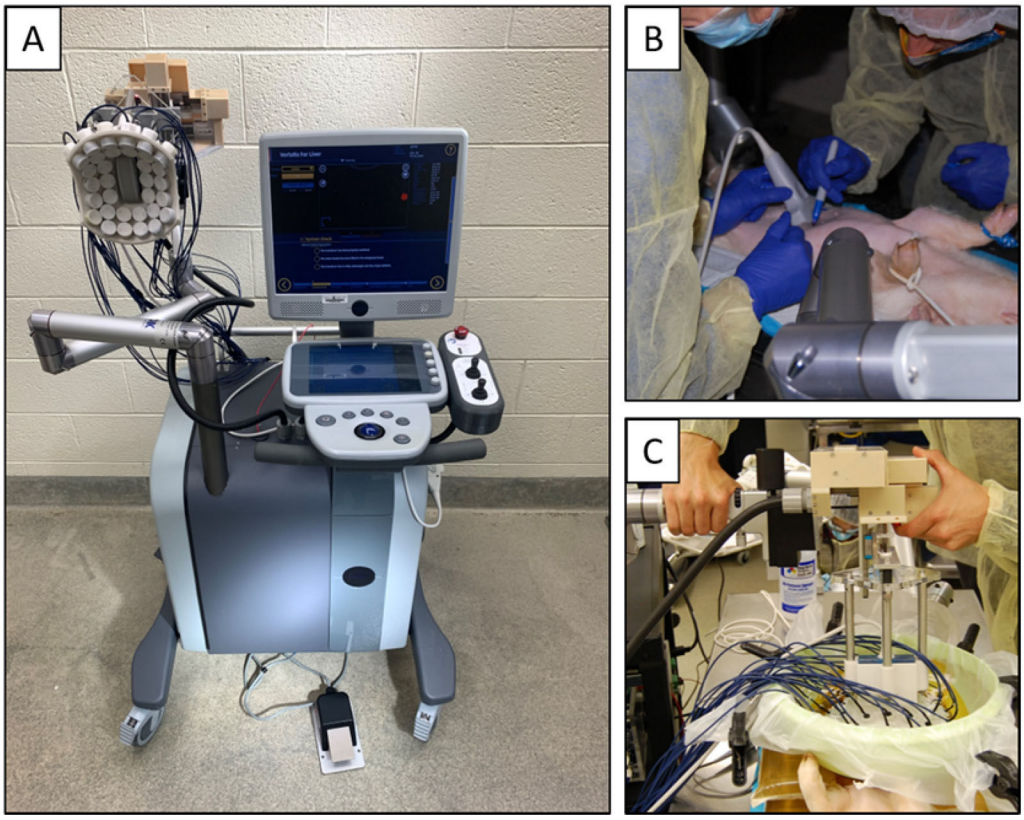


Figure 2.

Histotripsy Therapy System. Clinical histotripsy cart with 500 kHz transducer and coaxial US imaging probe mounted onto a micro-positioner (A) freehand imaging by a radiologist to identify acoustic window (B). UMC bowl with therapy transducer submerged *via* an adjustable arm (C).

Author Manuscript Author Manuscript Author Manuscript Author Manuscript

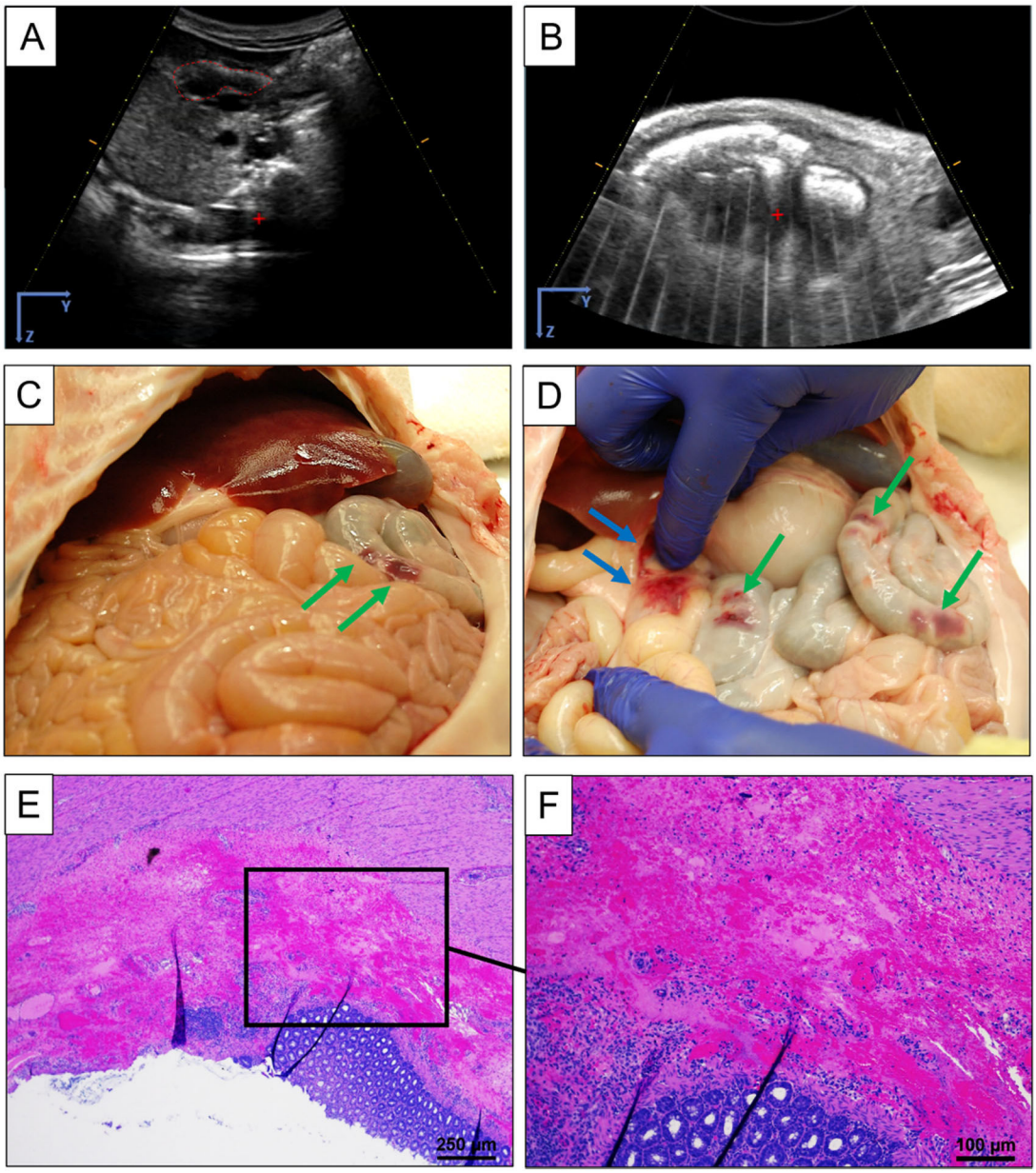


Figure 3.

Histotripsy Treatment - Fasted Acute Pigs. Freehand US imaging of pancreas body indicated by red dashed lines in a fasted pig (A). US imaging with standoff showing gas obstruction prior to histotripsy treatment (B). Intestinal gas interference with treatment prevented ideal imaging quality and bubble formation during treatment leading to pre-focal intestinal bruising (C-D) more highly concentrated in the more gaseous large intestine, indicated by the green arrow, and small intestine, indicated by the blue arrows. Post-treatment H&E histopathology indicated that from a sample of the bruised colon, the muscularis was not damaged but there was a large amount of ablation and hemorrhage within the submucosa (E-F).

Author Manuscript Author Manuscript Author Manuscript Author Manuscript

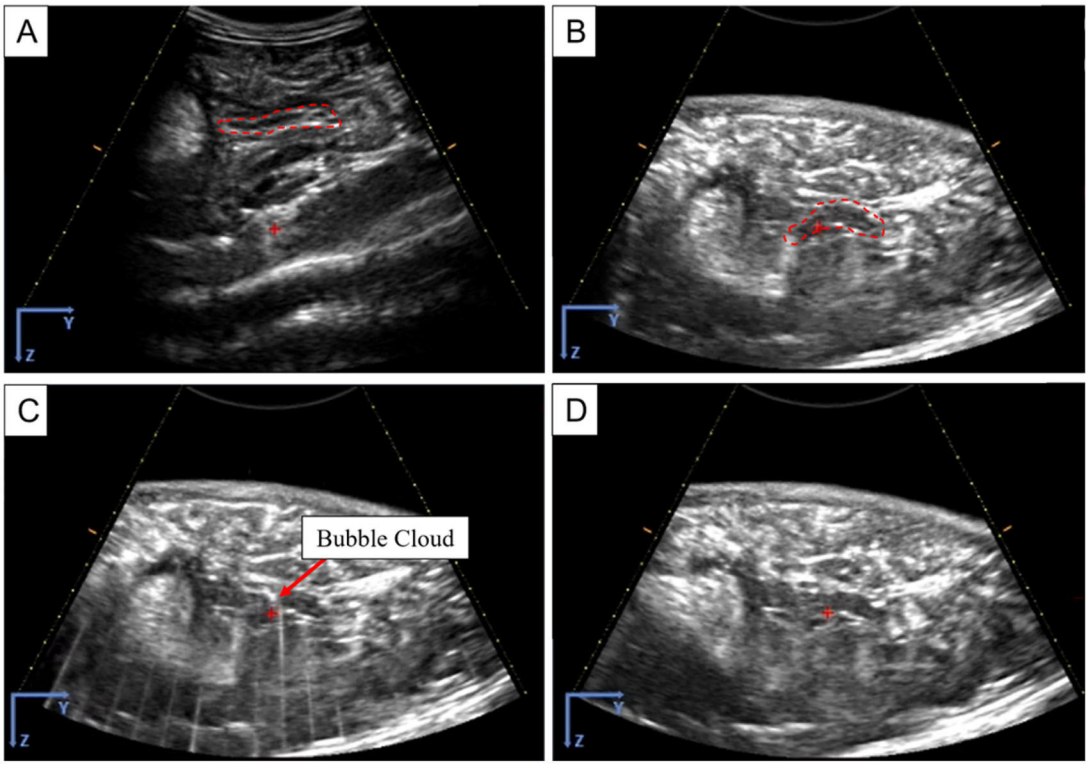


Figure 4.

Histotripsy Treatment - Specialty Diet Acute Pigs. Freehand US imaging of pancreas before histotripsy indicated by dashed lines (A). US image with standoff prior to treatment and ROI identified by dashed lines (B). US image during treatment of bubble cloud generated in the pancreas (C) and post-treatment (D). Supplementary Video S1.

Author Manuscript Author Manuscript Author Manuscript Author Manuscript

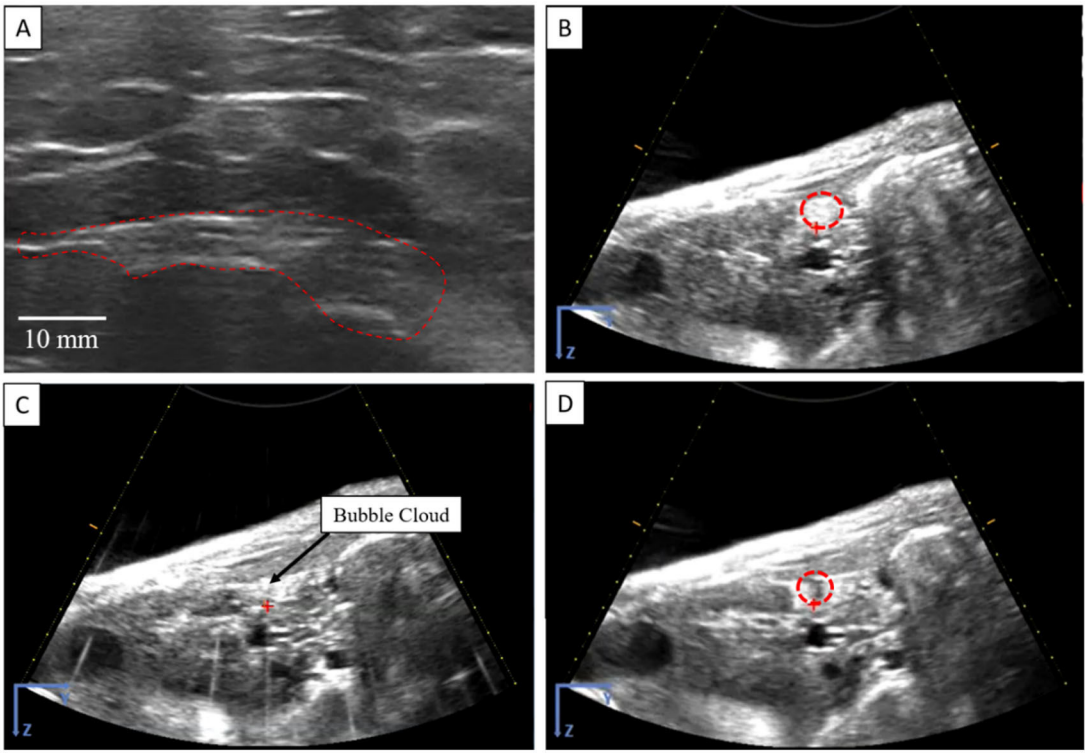


Figure 5.

Histotripsy Treatment - Specialty Diet Chronic Pigs. US imaging of the pancreas before histotripsy indicated by dashed lines (A). US image with standoff prior to treatment and target identified by the dashed red circle (B). US image during treatment of bubble cloud generated in the pancreas (C) and after treatment with a clear hypoechoic region identifying the targeted ablated volume (D). Dashed red circle indicated the approximate region treated. Supplementary Video S2.

Author Manuscript Author Manuscript Author Manuscript Author Manuscript

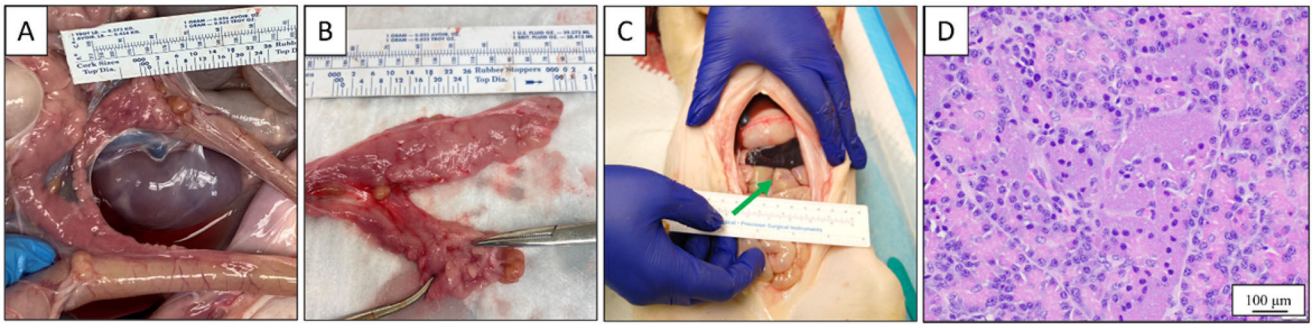


Figure 6.

Necropsy - Specialty Diet Acute Pigs. Necropsy revealed no gross damage within the abdomen *in situ* (A). When excised *in tota* no damage was found on the exterior of the pancreas (B), nor other organs (liver, spleen, intestines) not shown, representative of pigs SD-1 and SD-2. With laxative, simethicone, and custard pretreatment protocol, there was significantly less bruising in prefocal bowel (C) indicated by the green arrow. Bruising around the treatment area was more concentrated than on the bowel but was still less intense than in the pilot group for pig SD-4. Histological staining of the pancreas revealed some loss of pancreatic tissue architecture at the periphery of lobules with the expansion of the interlobular tissue by flocculent debris, representative of pigs SD-3 and SD-4(D).

Author Manuscript
Author Manuscript
Author Manuscript
Author Manuscript

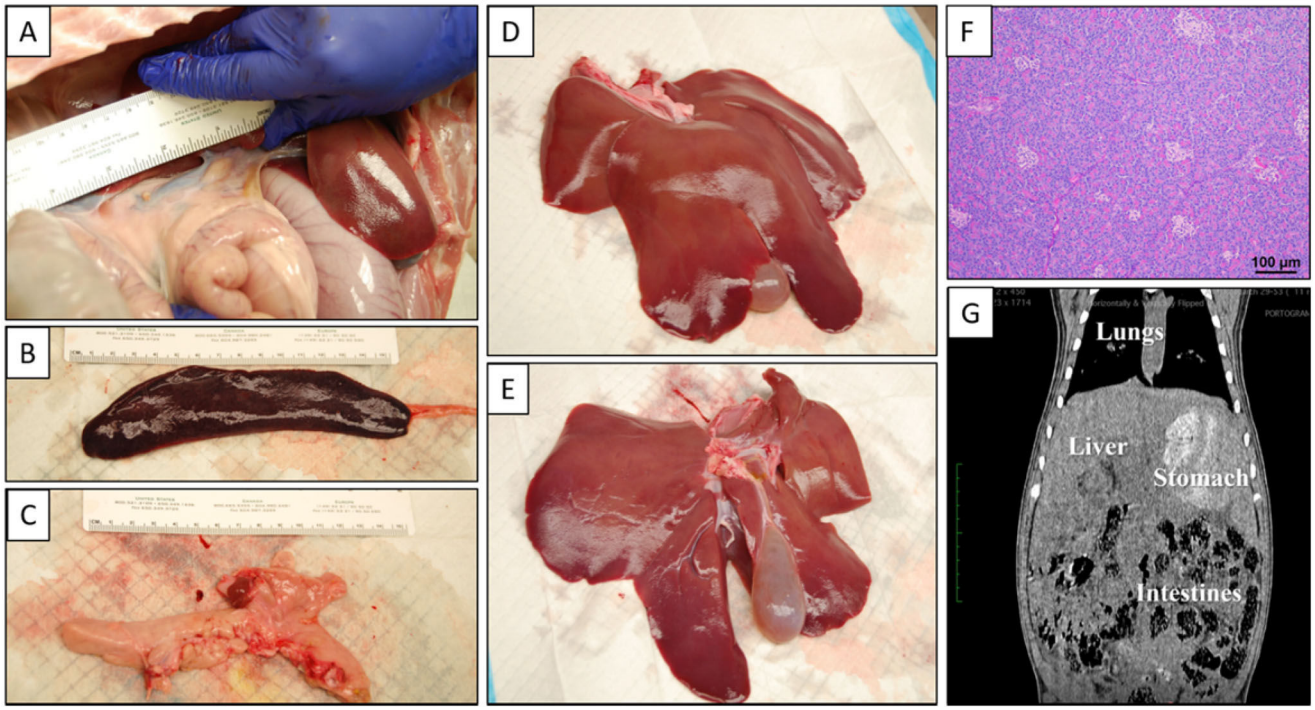


Figure 7.

Necropsy - Specialty Diet Chronic Pigs. Necropsy revealed no gross damage within the abdomen *in situ* (A). When excised *in tota* no damage was found on the exterior of the spleen (B), pancreas (C), nor liver (D-E). 1-week post-treatment showed no signs of morbidity within the pancreatic tissue (F) and CT did not show any indication of ablation or off-target damage (G).

Author Manuscript

Author Manuscript

Author Manuscript

Author Manuscript

Table 1.

Summary of all pig treatments. Note, regions of the pancreas visualized on US are in reference to the organ anatomy.

Group	Pig ID	Regions of pancreas visualized on US		Treatment peak negative pressure (MPa)	Focal bubble cloud in pancreas on US
		Freehand	Coaxial		
Acute	F-1	Portions of body	None	~21	No
	F-2	Portions of body to tail	None	~21	No
	F-3	Portion of tail	None	~21	No
	SD-1	Right side of body to head	Right side of body to head	~24	Yes
	SD-2	Right side of body to head	Right side of body to head	~24	Yes
	SD-3	Body to tail	None	~33–36	No
	SD-4	Body to tail	Body to tail	~41	Yes
Chronic	SD-5	Body to tail	Portions of body	~21	Yes
	SD-6	Portions of body	None	~19	No
	SD-7	Body to tail	None	~41	No
	SD-8	Body to tail	None	~41	No